Change in future climate due to Antarctic meltwater

Ben Bronselaer[1,2], Michael Winton[1], Stephen M. Griffies[1,3], William J Hurlin[1], Keith B. Rodgers[3], Olga V. Sergienko[1,3], Ronald J. Stouffer[1,2], Joellen Russell[2]

1. Geophysical Fluid Dynamics Laboratory, Princeton University Forrestal Campus, 201 Forrestal Road, Princeton, NJ 08540-6649, USA

2. Department Of Geosciences, University Of Arizona, Tucson, Arizona 85721, USA

3. Program in Atmospheric and Oceanic Sciences, Princeton University, Princeton, USA

Antarctic ice sheet melt is projected to cause up to 1m of sea level rise by 2100 under a high-emission RCP8.5 scenario. However, the effects of melt from the Antarctic ice sheet and shelves are not included in CMIP5 climate models, introducing bias into IPCC climate projections. Here we show that accounting for projected RCP8.5 Antarctic ice sheet meltwater in a large ensemble simulation of the CMIP5 model GFDL ESM2M delays 1.5°C and 2°C global mean atmospheric warming by more than a decade, causes enhanced drying of the Southern Hemisphere and reduced drying of the Northern Hemisphere, increases Antarctic sea-ice formation, and warms the sub-surface ocean around the Antarctic coast relative to the standard RCP8.5 scenario. Simulations with the ensemble that accounts for Antarctic meltwater are more consistent with recent observations of increasing Antarctic sea ice. The simulated ocean warming at 400m depth around the Antarctic coast caused by the ice melt

leads to a four-fold increase in ocean warming compared to the standard RCP8.5 scenario, possibly leading to further ice sheet/shelf melt through a positive feedback mechanism.

Observations have shown an acceleration in mass loss from the Antarctic ice sheet in recent years[1–3]. By the end of the 21st century, a recent study projects the Antarctic ice sheet to contribute almost 1m to global sea level rise under an RCP8.5 scenario[4], yet the latest generation of climate models taking part in the Coupled Model Intercomparison Project Phase 5 (CMIP5)[5] for the fifth IPCC Assessment report did not account for ice melt in future projections. Although output from model simulations is used to project sea level rise due to ice sheet mass loss, the feedback on the climate system is missing. Ice sheet and ice shelf melt will not be accounted for in the upcoming CMIP6 standard suite of experiments either[6].

Although the impact of the Antarctic ice sheet is most often considered in terms of global sea level[4,7], idealized climate model simulations show distinct effects of the meltwater flux on the simulated climate. In the Southern Ocean, the water mass stratification is such that a cold surface layer lies above a deep warm water layer called Circumpolar Deep Water (CDW). Ice sheet meltwater reduces ocean mixing and further isolates the warm CDW from the surface, which has been shown to cause cooling of sea surface temperatures and sub-surface ocean warming around Antarctica[8–10] and a potential expansion of sea ice[11,12]. This mechanism suggests that the cooling influence of meltwater released into the Southern Ocean can offset some of the 21st-century warming, delaying exceedance of the 2015 United Nations Climate Change Conference (COP21) warming targets[13]. Elevated sub-surface ocean temperature anomalies offshore can propagate into ice shelf cavities

and increase basal melting of ice shelves[11,14–17], although modeling studies disagree on the magnitude and impact of the climate response to Southern Ocean freshening[18,19,24]. In addition, this mechanism could alter atmospheric heat transport and rainfall patterns[20,21].

Here, we assess the impact of Antarctic meltwater on the climate state in a CMIP5 climate model simulation accounting for the historical and RCP8.5 projected ice sheet meltwater[4] (see Extended Data Fig. ED1) to show that modifications to a climate projection can be significant, indicating a current bias in our IPCC climate models. To do so, we use a large ensemble simulation between 1950 and 2100 of the CMIP5 model GFDL ESM2M (see Methods). The simulations that include the effect of ice sheet meltwater will be referred to as the "meltwater ensemble", whereas the simulations without meltwater are referred to as the "standard ensemble". By using a large ensemble simulation, we can robustly quantify the statistical significance of the effects of the meltwater on important aspects of the simulated climate and the time when the meltwater ensemble diverges from the standard ensemble.

To characterize the climate response to the release of Antarctic meltwater, we assess four key fields that are routinely used in IPCC assessments of climate change: surface air temperature, precipitation, sea ice cover, and the 400m depth ocean temperature around Antarctica. We include the sub-surface ocean temperature to highlight a possible feedback on ice shelf melting. The 400m depth is a representative depth for ocean temperature impact on ice shelves since this is the typical observed depth of warm circumpolar deep water from which intrusions onto the continental shelf are sourced[4]. For each of these four fields, we construct a metric: global mean surface air temper-

ature (SAT), the difference in precipitation between the Northern and Southern hemispheres as a measure of the shift in hemispheric rainfall (PRE), total Southern Hemisphere sea ice area (SHI), and the temperature anomaly around the Antarctic coast at 400m depth (ACT, taken as the temperature in the nearest 2 grid boxes from the coast). We demonstrate that the inclusion of ice-sheet meltwater reduces global atmospheric warming, causes a northwards shift in rainfall, an increase in sea ice area and an increase in the 400m offshore sub-surface Antarctic ocean temperature. We therefore show that ice sheet meltwater should be accounted for in climate models to improve our projections, since it is likely to affect policy targets.

1 Surface air temperature

The release of the meltwater around the Antarctic coast results in cooling of the surface ocean and overlying atmosphere relative to the RCP8.5 scenario (Fig. 1A). The largest temperature anomalies are simulated throughout the Southern hemisphere and extend into most of the Northern hemisphere, mitigating some of the warming due to the RCP8.5 greenhouse gas emissions throughout the globe.

Time evolution of the global SAT shows that this meltwater-induced cooling translates to a reduced rate of global warming (Fig. 1B). The maximum difference between the two ensembles (with and without the meltwater) is realized in the year 2055, when the meltwater-induced cooling is 0.38 ± 0.02°C.

The SAT response and the forcing curve (Fig. 1B) show that the SAT response is not linearly

related to the meltwater. Rather, the SAT response becomes weaker as the ocean becomes more stratified. The ocean stratifies due to both warming and freshening at the surface, such that the ice sheet meltwater has a weaker overall effect on the stratification as the ocean surface warms and the background convection is reduced (e.g. in the extreme case, if there is no ocean convection at all, any additional surface freshening has no further impact on convection).

2 Precipitation

Global changes in freshwater availability are determined by rainfall that can be characterized by changes in the position of Inter-Tropical Convergence Zone (ITCZ). The meltwater ensemble shows a northward shift of the ITCZ compared to the standard scenario, away from the hemisphere where meltwater is added (Fig. 2A), consistent with previous work[20,21]. These earlier studies have shown that additional freshwater release in the northern Atlantic Ocean causes a southwards shift in the ITCZ, towards the warmer hemisphere.

The ice sheet meltwater-induced precipitation change is strongest near the equator. The time evolution of the ITCZ position , shows a gradually increasing shift of the ITCZ toward the Northern Hemisphere in both the standard and meltwater ensembles (Fig. 2B). However, the measured ITCZ shift is stronger in the meltwater ensemble. Unlike the SAT anomaly, we find that the PRE anomaly changes linearly with meltwater flux (with $R^2 = 0.92$).

While the most intense precipitation changes are simulated over the ocean, there are changes in rainfall over land that generally follow the shift in the ITCZ: increased rainfall north of the

equator, and decreased rainfall in the Southern Hemisphere. The ice-melt induced precipitation changes can affect ENSO patterns, reduce drying of semi-arid regions in the Northern hemisphere (e.g. Central America, see Extended Data Fig. ED2) and increase drying South of the equator (e.g. Australia). Each change will have important consequences for agriculture and water scarcity.

3 Southern hemisphere sea ice area

The meltwater causes an increase in annual Southern Hemisphere sea ice area (SHI) relative to the standard RCP8.5 scenario (Fig. 3A) that is largely dominated by winter sea-ice anomalies (see Extended Data Fig. ED3). The maximum SHI anomaly is achieved in the year 2055. In this year, the mean SHI anomaly is $31 \pm 3\%$ of the pre-industrial annual averaged sea ice area. However, the SHI anomaly declines in the second half of the century. After the year 2060, the sea ice area reduces as the ocean surface continues to warm. At the end of the century, the meltwater ensemble projects almost no change in sea ice area compared to the 1950-1970 mean, as opposed to a 10% reduction in the ensemble without ice sheet melt.

The increase in SHI in the meltwater that peaks in the year 2055, begins at the start of the 21st century. This increase is in contrast to most climate model simulations, which show declining SHI[22], with the increase in line with the observed SHI trend over the 1979-2017 period (Fig. 3B). The reason for the observed trend is uncertain, because it could be explained, wholly or partly, by natural variability[23,24], forced atmospheric circulation changes[25,26] or increased freshwater input from ice shelves[11,26,27]. Over the period 1994-2012, the additional freshwater flux in the model

is 0.01 Sv (1 Sv = 10^6 m^3/s), compared to the observational estimate of 0.004-0.017 Sv[1,28–30]. The rate of change of the freshwater flux in the model is 0.0007 Sv yr^{-1} over this period, with observations estimating this flux at 0.0007-0.0013 Sv yr^{-1}. While the mean extra freshwater flux in the model over this period is in the middle of the observational range, the rate of change of the flux is at the low end.

The distributions of 1979-2017 linear trends in both the standard and meltwater ensembles and observations are shown in Fig. 3B. The standard ensemble has a weak mean trend ($0.000065 \pm 0.003 \times 10^6 km^2 yr^{-1}$), similar to the pre-industrial (prior to 1850) distribution of 39-year sea ice trends, as diagnosed from a 1500-year control simulation. The meltwater ensemble distribution of trends has a positive mean value of $0.015 \pm 0.007 \times 10^6 km^2 yr^{-1}$. Both ensembles can be considered consistent with observations, since the observed trend lies within the simulated range of natural variability of each. However, we find that the observational trend lies closer to the meltwater ensemble mean than the standard ensemble. Due to natural variability, we cannot attribute the observed sea ice trend to ice sheet meltwater flux, but the meltwater is likely to contribute. The meltwater ensemble simulates a large positive trend in sea ice area over the whole first half of the 21st century, so we cannot rule out a continued increase.

4 Antarctic coastal warming

The meltwater-induced sub-surface ocean warming around Antarctica, ACT (Fig. 4A) is highly concentrated along the coast in the Ross and Weddell seas, where the meltwater-induced warming

exceeds 3.5°C and 2.5°C, respectively. While time evolution of the ACT in the scenarios without ice sheet meltwater also shows sub-surface warming around the Antarctic coast[31] (Fig. 4B), the warming in the standard ensemble is a part of a widespread pattern of warming without enhanced warming around the coast. The sub-surface warming in the meltwater ensemble reaches a maximum at the end of the 21st century, increasing almost linearly with the strength of the meltwater flux.

The meltwater-induced ACT anomaly is mostly focused in the upper 1000m of the water column (Fig. 5A). The anomaly first appears at a maximum depth of 1250m, but as the atmosphere continues to warm and the meltwater flux increases, the maximum warming both increases in strength and shoals towards the surface. This is because the coastal meltwater-induced stratification changes become more confined to the surface. The heat flux anomalies that arise from the meltwater flux (see Extended Data Fig. ED4) are caused predominantly by eddy-induced isopycnal transport, i.e. advection and diffusion of heat by parametrized mesoscale eddies along surfaces of constant density[32]. Isopycnals are depressed near the Antarctic coast due to the surface freshening of the meltwater, causing transport of relatively warm circumpolar deep water towards the Antarctic coast continental shelf rather than towards the surface away from the shelf (see Fig. 5B).

The discharge of meltwater causes ocean warming at the depth where water masses are in contact with ice shelves. This warming can enable a positive feedback: warmer ocean waters increase sub-ice melting which in its turn leads to more meltwater and subsequently further sub-surface ocean warming[9,33,34]. This feedback has not been taken into account in the ref. 4 estimate

of ice sheet melt which uses ocean temperatures from a uncoupled ocean model.

5 Implications

Climate metrics (surface air temperature, hemispheric precipitation difference, Antarctic sea ice area and sub-surface coastal warming metrics) show significant alteration of future climate projections by accounting for the effects of Antarctic ice sheet meltwater. These alterations have consequences for climate policy and should be taken into account for future IPCC reports, given recent observational evidence of increasing mass loss from Antarctica[35]. A simulated COP21 global mean atmospheric warming target of 1.5°C, relative to the pre-industrial period, is first reached in the year 2037 in the standard scenario, but is first reached in the year 2050 in the meltwater ensemble. Similarly, 2°C of warming is first reached in 2053 in the standard scenario, but only in 2065 in the meltwater ensemble. However, this meltwater-induced reduction of transient climate warming occurs in tandem with the potential for enhanced sea level rise. These results emphasize the importance of the Southern Ocean response to ice sheet mass loss for estimates of 21st century climate change, thus identifying the need to account for meltwater effects in climate projections. The direct contribution from Antarctic ice sheet mass loss is already included in the IPCC assessments of future sea level rise, although it was acknowledged to be highly uncertain in the fifth assessment report. The climate impact is missing however, even in the upcoming CMIP6 experimental design. Similarly, the effects of Greenland ice sheet melt have so far also not been considered, and could lead to further changes in simulated future climate[8,36].

We identify a physical mechanism whereby increased meltwater could lead to heat transport enhanced by eddies into Antarctic sub-ice-shelf cavities, enabling a positive feedback. Although our model does not resolve ice shelf cavities, we can estimate the future magnitude of this positive feedback on ice shelf melt using the parameterization from ref. 4 (see Methods). Meltwater-induced ocean warming could result in a 9-34% increase in Southern Ocean meltwater flux from increased ice shelf melt (see Extended Data Fig. ED5), even when we consider the possibility of lower meltwater flux. This feedback could potentially increase sea level further by causing an increased ice flux across the grounding line. Such a feedback mechanism is supported by paleo evidence[19,37]. However, the Southern Ocean is a complex system and many ice sheet-related feedbacks need to be accounted for, such as atmospheric heat and moisture transport, surface heat fluxes, ice-shelf cavity dynamics and sea-ice changes[21,38,39]. Global coupled models such as ESM2M are useful tools for identifying and quantifying the potential of this feedback by modeling the Southern Ocean temperature response and accounting for global feedbacks that process-based models cannot capture, but lack high-resolution contintental shelf and ice-shelf cavity dynamics. However, this is a challenging problem and global coupled model simulations need to be complemented with regional ice sheet studies to fully constrain the magnitude of the ice loss feedback. The most recent modeled estimate of the Antarctic contribution towards global sea level in 2100 is 0.86 m[4], but considering feedbacks like the meltwater-induced ocean warming, this number could be higher.

While this paper mainly discusses the changes of the ensemble mean climate state by the inclusion of ice sheet meltwater, the time series in Figs. 1B, 2B, 3A, and 4B show the period

during which the meltwater signal would be significant in a single climate simulation, for example a single submission to CMIP6. For the SAT, SHI and ACT metrics, this period is most of the 21st century, showing the distinct climate impact of the ice sheet melt over natural variability, and the importance of including the associated meltwater flux in all simulations. While coupling ice sheet models to climate models remains challenging, we recommend adding projected meltwater flux as a feasible intermediate step, although this is not mass-conserving.

There are several caveats in our experimental design. We impose the meltwater flux in a spatially uniform pattern around the coast at the surface of the ocean, without partitioning into liquid meltwater and solid icebergs. A previous study shows that most of meltwater input from icebergs occurs within our meltwater flux region around the Antarctic coast[40], justifying the neglect of iceberg meltwater injection. Ice sheet mass loss is also not uniform[1,41]. However, it is unclear if the spatially uniform injection of meltwater affects the climate impact of the meltwater[42,43] (see Methods). We add the meltwater at the surface even though some will be discharged at depth due to basal melt, which might affect regional sea ice trends[26], but total Antarctic sea ice area and sea surface temperature trends are not significantly affected[30]. Further research with coupled ice-ocean-atmosphere models should therefore focus on constraining the effect of meltwater-induced sub-surface ocean warming on ice-shelf melt. While observed sea ice trends are also highly regional and likely dependent on the spatial distribution of the sea-ice melt[26], our uniform flux is appropriate for analyzing total sea-ice area[30]. We also only use one climate model and we expect the quantitative results to be model dependent, including estimates of the meltwater feedback mechanism discussed above[8,44]. However, the large-scale ocean and atmospheric mechanisms of

the response to the Antarctic meltwater discharge shown here should be robust because the mechanisms are consistent with previous studies[8,9,18,19,45]. The multi-model response should be assessed through efforts such as the Southern Ocean Modeling Intercomparison Project (SOMIP) [46] and Flux-anomaly-forced model intercomparison project (FAFMIP) [47].

Conclusions

Our study, focused on accounting for the effects of Antarctic ice sheet meltwater on the rest of the climate system using large ensemble RCP8.5 climate change simulations, finds that the effects are significant and that the meltwater discharge plays an important role in determining the climate state of the 21st century. It causes a reduction in global atmospheric warming, delaying 1.5° and 2° warming targets by over 10 years; it drives a northwards shift of the Inter-Tropical Convergence Zone, resulting in reduced drying over Northern Hemisphere landmasses and enhanced drying in the Southern Hemisphere; it causes a significant (maximum 31%) increase in Antarctic sea-ice formation, relative to the pre-industrial period; and a fourfold increase in warming of the subsurface ocean around the Antarctic coast. Our results suggest an operation of a feedback mechanism whereby the meltwater-induced subsurface warming could lead to enhanced sub-ice-shelf melting, potentially causing further meltwater-related climate effects. These results demonstrate for the first time that meltwater discharge from the Antarctic ice sheet not only contributes to sea level rise but also influences the global climate throughout most of the 21st century, emphasizing the importance of ocean and ice-sheet feedbacks on the climate system. Antarctic meltwater therefore represents an important agent of climate change with global impact, likely affecting climate policy,

and should be taken into account in future climate simulations.

1. Paolo, F. S., Fricker, H. A. & Padman, L. Volume loss from Antarctic ice shelves is accelerating. Science **348**, 327-331 (2015).

2. Wouters, B. et al. Dynamic thinning of glaciers on the Southern Antarctic Peninsula. Science **348**, 899-903 (2015).

3. Konrad, H. et al. Net retreat of Antarctic glacier grounding lines. Nature Geoscience **11**, 258-262 (2018).

4. DeConto, R. M. & Pollard, D. Contribution of Antarctica to past and future sea-level rise. Nature **531**, 591-597 (2016).

5. Taylor, K. E., Stouffer, R. J. & Meehl, G. A. An Overview Of CMIP5 And The Experiment Design. Bulletin Of The American Meteorological Society **93**, 485-498 (2012).

6. Eyring, V. et al. Overview of the Coupled Model Intercomparison Project Phase 6 (CMIP6) experimental design and organization. Geoscientific Model Development **9**, 1937-1958 (2016).

7. Rignot, E., Velicogna, I., van den Broeke, M. R., Monaghan, A. & Lenaerts, J. Acceleration of the contribution of the Greenland and Antarctic ice sheets to sea level rise. Geophysical Research Letters **38**, L05503 (2011).

8. Stouffer, R. J., Seidov, D. & Haupt, B. J. Climate response to external sources of freshwater: North Atlantic versus the Southern Ocean. Journal of Climate **20**, 436-448 (2007).

9. Fogwill, C. J., Phipps, S. J., Turney, C. S. M. & Golledge, N. R. Sensitivity of the Southern Ocean to enhanced regional Antarctic ice sheet meltwater input. Earths Future **3**, 317-329 (2015).

10. Park, W. & Latif, M. Ensemble Global Warming Simulations with idealized Antarctic Meltwater. Climate Dynamics (2018).

11. Bintanja, R., van Oldenborgh, G. J., Drijfhout, S. S., Wouters, B. & Katsman, C. A. Important role for ocean warming and increased ice-shelf melt in Antarctic sea-ice expansion. Nature Geoscience **6**, 376-379 (2013).

12. Pauling, A. G., Smith, I. J., Langhorne, P. J. & Bitz, C. M. Time-Dependent Freshwater Input From Ice Shelves: Impacts on Antarctic Sea Ice and the Southern Ocean in an Earth System Model. Geophysical Research Letters **44**, 10454-10461 (2017).

13. Rhodes, C. J. The 2015 Paris Climate Change Conference: COP21. Science Progress **99**, 97-104 (2016).

14. Oppenheimer, M. Global warming and the stability of the West Antarctic Ice Sheet. Nature **393**, 325-332 (1998).

15. Rignot, E. & Jacobs, S. Rapid bottom melting widespread near Antarctic ice sheet grounding lines. Science **296**, 2020-2023 (2002).

16. Shepherd, A., Wingham, D. & Rignot, E. Warm ocean is eroding West Antarctic Ice Sheet. Geophysical Research Letters **31**, L23402 (2004).

17. Obase, T., Abe-Ouchi, A., Kusahara, K., Hasumi, H. & Ohgaito, R. Responses of Basal Melting of Antarctic Ice Shelves to the Climatic Forcing of the Last Glacial Maximum and CO2 Doubling. Journal of Climate **30**, 3473-3497 (2017).

18. Aiken, C. M. & England, M. H. Sensitivity of the present-day climate to freshwater forcing associated with Antarctic sea ice loss. Journal of Climate **21**, 3936-3946 (2008).

19. Bakker, P., Clark, P. U., Golledge, N. R., Schmittner, A. & Weber, M. E. Centennial-scale Holocene climate variations amplified by Antarctic Ice Sheet discharge. Nature **541**, 72-76 (2017).

20. Zhang, R. & Delworth, T. Simulated tropical response to a substantial weakening of the Atlantic thermohaline circulation. Journal Of Climate **18**, 1853-1860 (2005).

21. Cabre, A., Marinov, I. & Gnanadesikan, A. Global Atmospheric Teleconnections and Multi-decadal Climate Oscillations Driven by Southern Ocean Convection. Journal of Climate **30**, 8107-8126 (2017).

22. Purich, A., Cai, W., England, M. H. & Cowan, T. Evidence for link between modelled trends in Antarctic sea ice and underestimated westerly wind changes. Nature Communications **7**, 10409 (2016).

23. Polvani, L. M. & Smith, K. L. Can natural variability explain observed Antarctic sea ice trends? New modeling evidence from CMIP5. Geophysical Research Letters **40**, 3195-3199 (2013).

24. Swart, N. C. & Fyfe, J. C. The influence of recent Antarctic ice sheet retreat on simulated sea ice area trends. Geophysical Research Letters **40**, 4328-4332 (2013).

25. Haumann, F. A., Notz, D. & Schmidt, H. Anthropogenic influence on recent circulation-driven Antarctic sea ice changes. Geophysical Research Letters **41**, 8429-8437 (2014).

26. Merino, N. et al. Impact of increasing antarctic glacial freshwater release on regional sea-ice cover in the Southern Ocean. Ocean Modelling **121**, 76-89 (2018).

27. Bintanja, R., Van Oldenborgh, G. J. & Katsman, C. A. The effect of increased fresh water from Antarctic ice shelves on future trends in Antarctic sea ice. Annals of Glaciology **56**, 120-126 (2015).

28. Shepherd, A. et al. A Reconciled Estimate of Ice-Sheet Mass Balance. Science **338**, 1183-1189 (2012).

29. Sutterley, T. C. et al. Mass loss of the Amundsen Sea Embayment of West Antarctica from four independent techniques. Geophysical Research Letters **41**, 8421-8428 (2014).

30. Pauling, A. G., Bitz, C. M., Smith, I. J. & Langhorne, P. J. The Response of the Southern Ocean and Antarctic Sea Ice to Freshwater from Ice Shelves in an Earth System Model. Journal of Climate **29**, 1655-1672 (2016).

31. Goddard, P. B., Dufour, C. O., Yin, J., Griffies, S. M. & Winton, M. CO2-Induced Ocean Warming of the Antarctic Continental Shelf in an Eddying Global Climate Model. Journal of Geophysical Research-Oceans **122**, 8079-8101 (2017).

32. Stewart, A. L. & Thompson, A. F. Eddy-mediated transport of warm Circumpolar Deep Water across the Antarctic Shelf Break. Geophysical Research Letters **42**, 432-440 (2015).

33. Silvano, A. et al. Freshening by glacial meltwater enhances melting of ice shelves and reduces formation of Antarctic Bottom Water. Science Advances **4**, eaap9467 (2018).

34. Spence, P. et al. Localized rapid warming of West Antarctic subsurface waters by remote winds. Nature Climate Change **7**, 595-603 (2017).

35. Shepherd, A. et al. Antarctic ice shelf disintegration triggered by sea ice loss and ocean swell. Nature, 383-389 (2018).

36. Vizcaino, M. et al. Coupled simulations of Greenland Ice Sheet and climate change up to AD 2300. Geophysical Research Letters **42**, 3927-3935 (2015).

37. Sangiorgi, F. et al. Southern Ocean warming and Wilkes Land ice sheet retreat during the mid-Miocene. Nature Communications **9**, 317 (2018).

38. Fyke, J., Sergeinko, O., Loftverstorm, M., Price, S. & Lenaerts, J. T. M. An Overview of Interactions and Feedbacks Between Ice Sheets and the Earth System. Reviews of Geophysics, 361-408 (2018).

39. Massom, R. A. et al. Antarctic ice shelf disintegration triggered by sea ice loss and ocean swell. Nature, 383-389 (2018).

40. Stern, A. A., Adcroft, A. & Sergienko, O. The effects of Antarctic iceberg calving- size distribution in a global climate model. Journal Of Geophysical Research-Oceans **121**, 5773-5788 (2016).

41. Rignot, E., Jacobs, S., Mouginot, J. & Scheuchl, B. Ice-Shelf Melting Around Antarctica. Science **341**, 741-756 (2013).

42. Stammer, D. Response of the global ocean to Greenland and Antarctic ice melting. Journal of Geophysical Research-Oceans **113**, C06022 (2008).

43. Haid, V., Iovino, D. & Masina, S. Impacts of freshwater changes on Antarctic sea ice in an eddy-permitting sea-ice-ocean model. Cryosphere **11**, 1387-1402 (2017).

44. He, J., Winton, M., Vecchi, G., Jia, L. & Rugenstein, M. Transient Climate Sensitivity Depends on Base Climate Ocean Circulation. Journal Of Climate **30**, 1493-1504 (2017).

45. Swingedouw, D., Fichefet, T., Goosse, H. & Loutre, M. F. Impact of transient freshwater releases in the Southern Ocean on the AMOC and climate. Climate Dynamics **33**, 365-381 (2009).

46. SOMIP. http://southernocean.arizona.edu/node/10896 (2016).

47. Gregory, J. M. et al. The Flux-Anomaly-Forced Model Intercomparison Project (FAFMIP) contribution to CMIP6: investigation of sea-level and ocean climate change in response to CO2 forcing. Geoscientific Model Development **9**, 3993-4017 (2016).

48. Fetterer, F., Knowles, K., Meier, W., Savoie, M. & Windnagel, A. K. Sea Ice Index, Version 3: Sea Ice Extent. Boulder, Colorado USA. NSIDC: National Snow and Ice Data Center. Date Accessed: 03/01/2018 (2017).

Acknowledgements This work was sponsored by NSF's Southern Ocean Carbon and Climate Observations and Modeling (SOCCOM) Project under the NSF Award PLR-1425989, with additional support from NOAA and NASA. OS is supported by NSF OPP-1246151 and by awards NA14OAR4320106 and NA13OAR431009 from the National Oceanic and Atmospheric Administration, U.S. Department of Commerce. The statements, findings, conclusions, and recommendations are those of the author and do not necessarily reflect the views of the National Oceanic and Atmospheric Administration, or the U.S. Department of Commerce. We thank Jorge Sarmiento, Jianjun Yin and Alex Haumann for their insight.

Author Information Reprints and permissions information is available at www.nature/com/reprints. The authors declare no competing interests. Correspondence and requests for materials should be addressed to B.B. (benjamin.bronselaer@noaa.gov).

Author Contributions B.B. performed the simulations with help from W.J.H., M.W., R.J.S. and K.B.R.; B.B., M.W., and J.R. analyzed the data with help from R.J.S. (climate response to ocean meltwater input), S.M.G. (ocean dynamics and heat budget) and O.V.S. (ice-ocean interactions and feedbacks); M.W. and J.R. supervised the project. All authors wrote the manuscript.

Reviewer Information We thank the editor, Michael White, and two anonymous reviewers for their comments and contributions towards peer review.

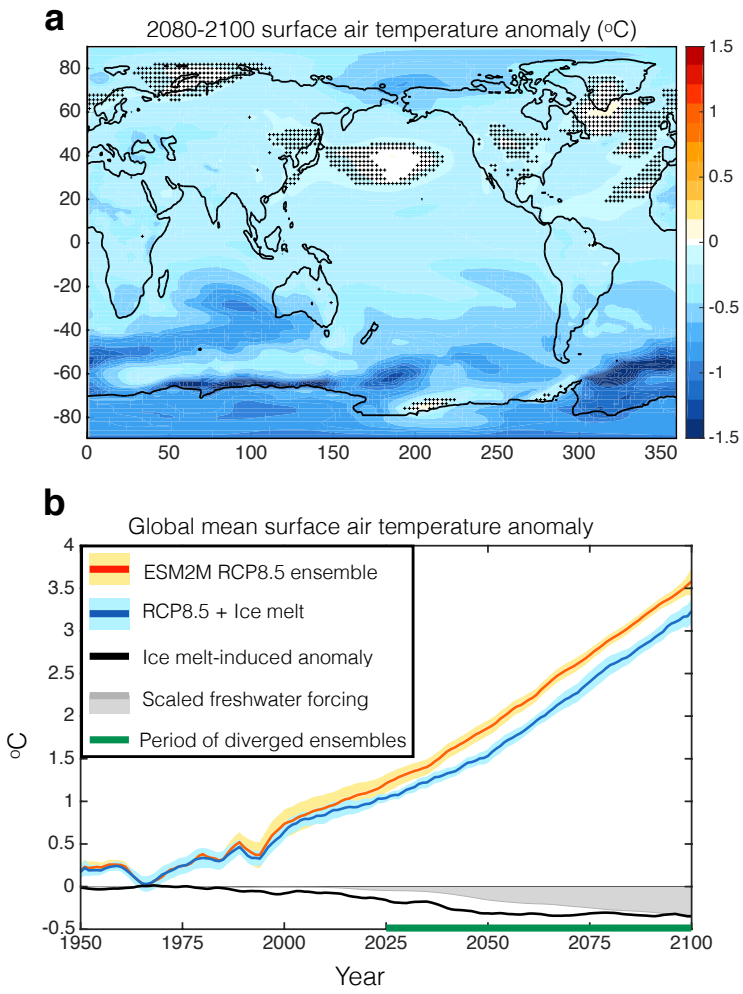

Figure 1: **Surface air temperature anomalies**: **a**, 2080-2100 meltwater-induced surface air temperature (SAT) anomaly relative to the standard scenario. Hatching indicates where the anomalies are not significant at the 95% level. **b**, Time series of the global mean surface air temperature anomaly relative to the 1950-1970 mean. Orange shows the standard ensemble and blue shows the meltwater ensemble. Solid lines show ensemble means, the dark shading shows the uncertainty in the mean and the light shading shows the full ensemble spread of 20-year SAT means. In this case, the dark shading envelope is too narrow to be visible. The solid black line shows the difference between the orange and blue lines, and the applied meltwater flux is shown in grey (scaled to the final 5-year mean of the meltwater-induced SAT anomaly). The green bar indicates when the full ensembles have diverged.

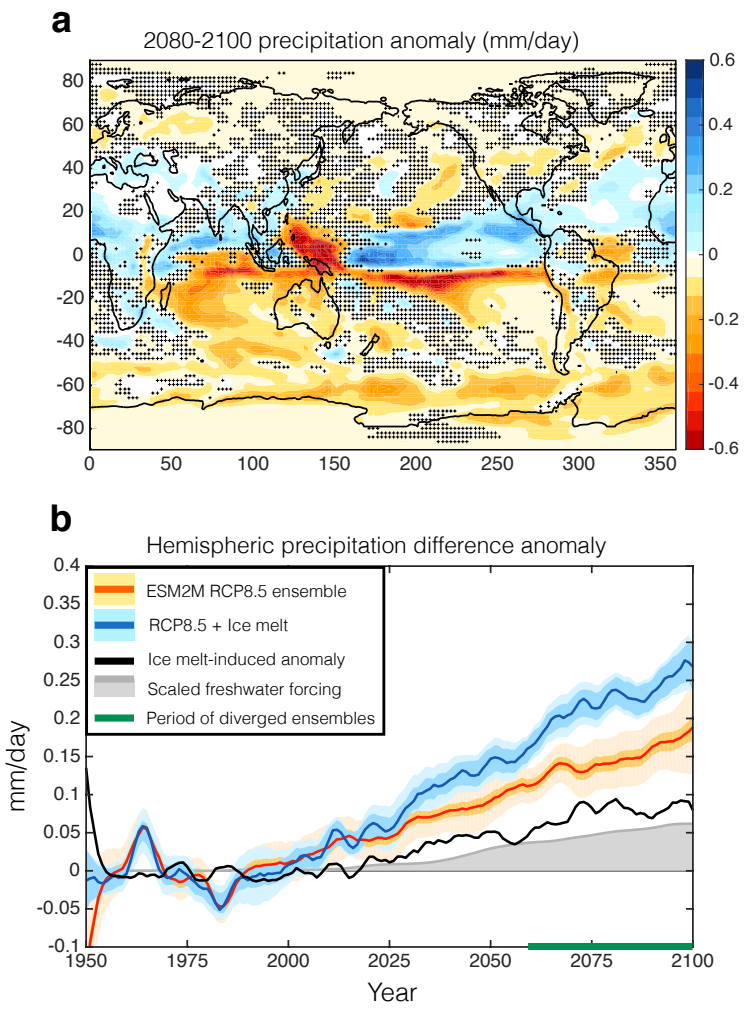

Figure 2: **Precipitation anomalies**: **a**, 2080-2100 meltwater-induced precipitation anomaly relative to the standard scenario. Hatching indicates where the anomalies are not significant at the 95% level. **b**, Time series of the North-South hemispheric precipitation difference (PRE) anomaly relative to the 1950-1970 mean. Orange shows the standard ensemble and blue shows the meltwater ensemble. Solid lines show ensemble means, the dark shading shows the uncertainty in the mean and the light shading shows the full ensemble spread of 20-year PRE means. The solid black line shows the difference between the orange and blue lines, and the applied meltwater flux is shown in grey (scaled to the final 5-year mean of the meltwater-induced PRE anomaly). The green bar indicates when the full ensembles have diverged.

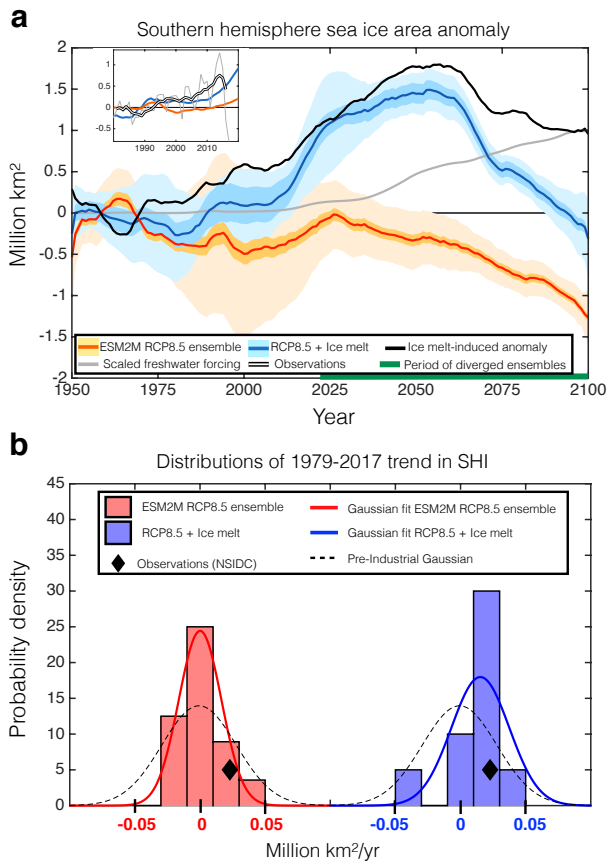

Figure 3: **Sea ice anomalies**: **a**, Time series of the annual mean Southern Hemisphere sea-ice (SHI) anomaly relative to the 1950-1970 mean. Orange shows the standard ensemble and blue shows the meltwater ensemble. Solid lines show ensemble means, the dark shading shows the uncertainty in the mean and the light shading shows the full ensemble spread of 20-year means. The solid black line shows the difference between the orange and blue lines, and the applied meltwater flux is shown in grey (scaled to the final 5-year mean of the meltwater-induced SHI anomaly). The green bar indicates when the full ensembles have diverged. The insert panel shows the 1980-2020 period with the double black line showing observed sea ice area from the National Snow and Ice Data Center[48], relative to the 1980-2000 mean. The thin grey line shows the unsmoothed observations. **b**, Distribution of linear trends in SHI over the period 1979-2017, calculated for each ensemble member. The red bars show the standard ensemble and blue bars show the meltwater ensemble, with different x-axes. The solid lines show Gaussian fits to the distributions, and the dashed black line shows the pre-industrial distribution. The observations are shown in black diamonds.

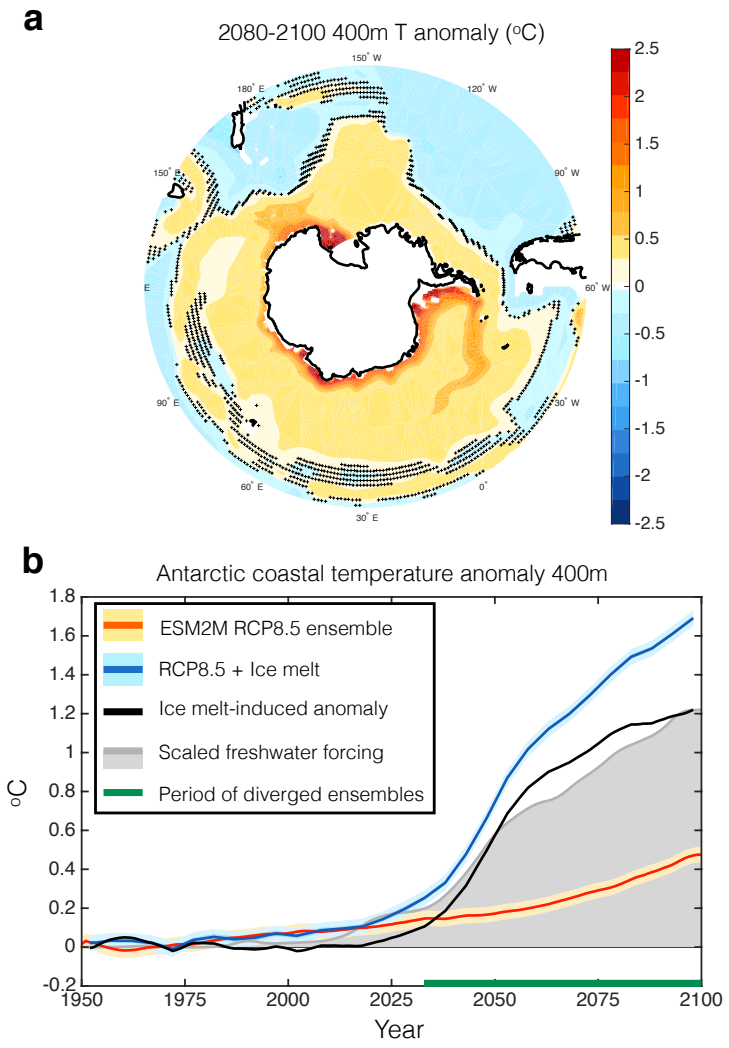

Figure 4: **Ocean warming**: **a**, 2080-2100 meltwater-induced anomaly of the ocean temperature around the Antarctic coast at 400m depth relative to the standard scenario. Hatching indicates where the anomalies are not significant at the 95% level. **b**, Time series of the anomaly in the ocean temperature around the Antarctic coast at 400m depth (ACT) relative to the 1950-1970 mean. Orange shows the standard ensemble and blue shows the meltwater ensemble. Solid lines show ensemble means, the dark shading shows the uncertainty in the mean and the light shading shows the full ensemble spread of 20-year ACT means. In this case, the dark shading envelope is too narrow to be visible. The solid black line shows the difference between the orange and blue lines, and the applied meltwater flux is shown in grey (scaled to the final 5-year mean of the meltwater-induced ACT anomaly). The green bar indicates when the full ensembles have diverged.

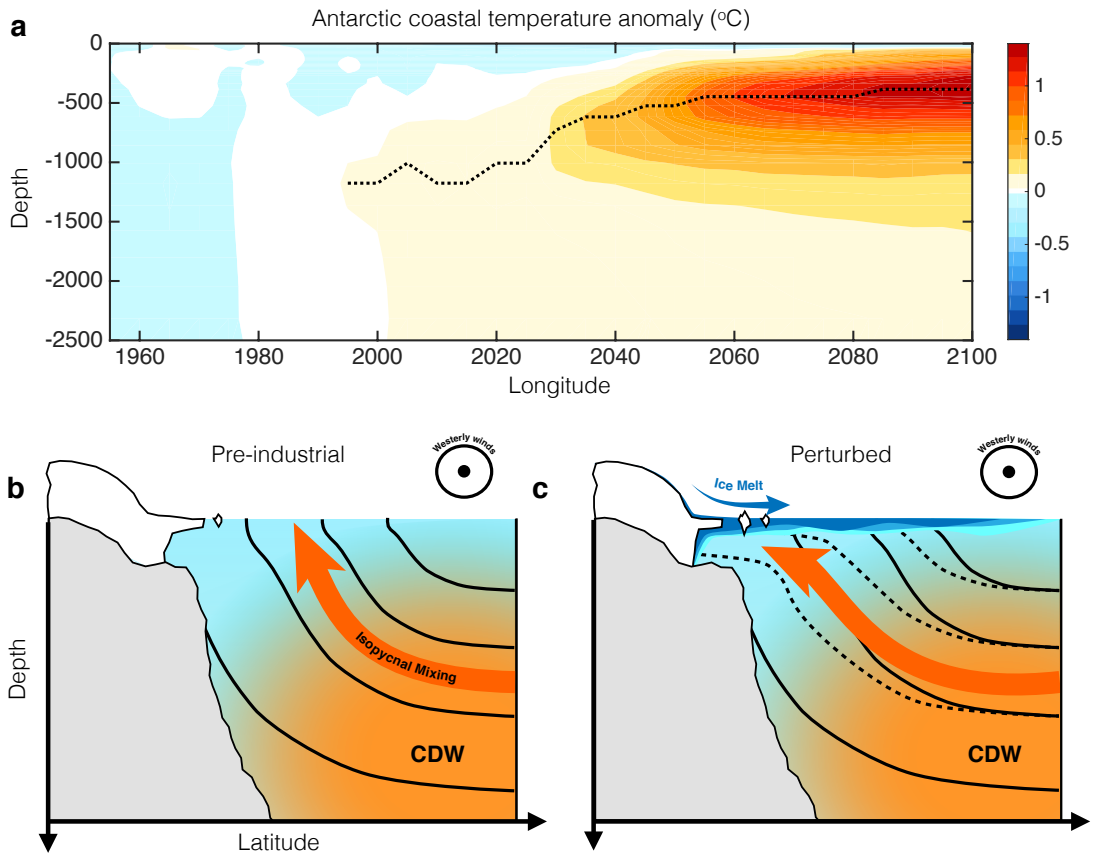

Figure 5: **Ocean warming mechanism**: **a**, Hovmoller diagram of the meltwater-induced ocean temperature anomaly, averaged along the Antarctic coast, as a function of time. The black dots indicate the depth of maximum warming. Panels **b** and **c**, schematic of the meltwater-induced Southern Ocean subsurface warming, shown as a zonal mean section: In the pre-industrial state (panel **b**), isopycnals are tilted towards the ocean's surface away from the continental shelf with an upward heat flux transporting heat from the warm CDW at depth towards the surface. In the perturbed state (panel **c**), Antarctic ice melt freshens the surface, depressing isopycnals such that the isopycnal mixing transports heat towards the continent rather than towards the ocean's surface, leading to coastal warming at depth around the shelf (red circle) and cooling at the surface (blue circle).

Methods

Ice-melt freshwater flux projection To represent Antarctic ice sheet meltwater, we apply an external source of freshwater to the climate model. We use the time series of yearly freshwater flux representing Antarctic ice sheet and shelf melt from ref. 4, by digitization from their Extended Data Figure 8. The error in total applied freshwater flux arising from the digitization in year 2100 is 1.3% (see Extended Data Fig. ED1), which is negligible in the context of our study (the difference in the response in the 400m Antarctic coastal temperature to 200% or 50% the ref. 4 flux is only roughly $\pm 25\%$, as discussed in the "Estimation of sub-surface warming feedback"section below). This flux includes the freshwater input from both melting of the grounded ice sheet and the floating ice shelves. The flux includes contributions from basal melt, grounding-line retreat, surface meltwater and rain runoff, surface and basal calving, crevassing and hydrofracturing. The freshwater flux gives the total ice sheet volume change, which accounts for accumulation of precipitation over the Antarctic continent as the climate warms. This precipitation change is also simulated in ESM2M, resulting in a double counting. However, the ensemble mean simulated cumulative precipitation change over Antarctica in 2100 in the ESM2M RCP8.5 standard ensemble is 1% of the total freshwater flux and therefore negligible.

Throughout this paper, we refer to both ice sheet and ice shelf melt. The ice sheet melt refers to the meltwater from grounded ice, and ice shelf melt refers to the meltwater from floating ice. While it is the total freshwater flux that is relevant for the climate response to the ice melt, it is only the ice sheet melt that will contribute towards global mean sea level rise (roughly half of the total

freshwater input). The global mean sea level rise equivalent for the prescribed freshwater flux is therefore higher than the quoted global mean sea level rise in ref. 4. The ice sheet model used in ref. 4 uses a 10km horizontal resolution coupled to a regional atmospheric model. Ocean temperatures for basal melt in that study were taken from the 400m depth level from a de-coupled RCP8.5 simulation performed with the NCAR CCSM4[49]. The model was forced with total equivalent atmospheric CO_2, accounting for the contributions from radiatively active trace gases.

GFDL ESM2M The model employed in this study is the GFDL ESM2M. ESM2M is a CMIP5 Earth System model with a full carbon cycle at $1 \times 1^{\circ}$ horizontal ocean model resolution with increased resolution near the equator and 50 unevenly spaced vertical levels in depth coordinates, with a free surface[50,51] and parameterized mesoscale eddies using the GM-Redi schemes[52]. ESM2M does not have interactive ice sheets, so ice sheet and shelf melt need to be prescribed as freshwater flux. The Transient Climate Response (TCR) of ESM2M is 1.5K, which is at the low end of the CMIP5 models[53]. The Southern Ocean in ESM2M has relatively deep mixed layers compared to the overall CMIP5 mean, resulting from a slightly more convective mean state relative to the CMIP5 mean, but it is not an outlier within the CMIP5 ensemble[54]. The ESM2M mean state could impact the magnitude of the model's response to freshwater flux compared to other models[44].

The response of the mean Southern Ocean mixed layer depth to future climate change scenarios (both RCP4.5 and RCP8.5) is weak compared to the CMIP5 mean[54]. The mean state Antarctic sea ice area is low compared to observations[55]. The ESM2M negative historical (1979-2013) trend

in Antarctic summer and winter sea ice extent and Southern Ocean sea surface temperature warming (SST) south of 55°S is weaker than average[22]. ESM2M simulates summertime cooling of Southern Ocean SSTs over the 1979-2013 period, while most other models simulate warming[22]. Although ESM2M is on the convective side of CMIP5 models, the sea ice volume varies only weakly with rate of Southern Ocean convection[56]. Ref. 54 shows that there is a large spread in winter-time mixed layer patterns and convection. However, ESM2M has deep mixed layers in areas which correspond to the observations. Winter-time open-ocean convection and polynya formation in ESM2M is confined to the Eastern Weddell sea[54], similar to observed open-ocean polynya's in the 1970's and in recent years[57,58]. Observations also show deep mixed layers around the Antarctic coast where dense water is thought to form. ESM2M also simulates deeper mixed layers around the coast, however, these mixed layers in ESM2M are shallower than observed[59]. CMIP5 models are also known to have Southern Ocean Westerly winds that are too far equatorward[60]. However, ESM2M has one of the smallest biases in Southern Ocean wind position and strength within CMIP5 models[61]. Moreover, ESM2M has been shown to perform well in terms of global and Southern Ocean heat uptake[62]. The density structure of ESM2M around the Antarctic coast is compared to the Southern Ocean State Estimate (SOSE)[63] in the section "ESM2M Southern Ocean Evaluation".

Experimental design To simulate melting of the Antarctic land ice, we add an external source of freshwater at the ocean's surface to 10 ensemble members, similar to previous studies[8]. The additional freshwater is added at sea surface temperature. The freshwater perturbation does not have a seasonal cycle, and is added uniformly around the Antarctic continent, in the three grid

boxes against the coast (corresponding to 3 degrees in latitude away from the coastline). While we impose all of the freshwater at the ocean's surface for ease of reproduction, part of this melt is due to basal melting, which would be deposited in the ocean at several hundred meters depth. Ref. 30 show that putting all the freshwater flux at depth compared to all at the surface affects the local mixed layer response, but does not significantly affect total Antarctic sea ice trends. Adding the freshwater at depth does increase the magnitude of the sub-surface warming[30]. On the other hand, ref. 30 show that the depth of freshwater flux does affect regional sea ice trends. For these reasons, we acknowledge that adding all the freshwater at the surface is a limitation, but one which is unlikely to significantly affect the climate metrics discussed in this paper, apart from the sub-surface warming which may be underestimated.

We also add the freshwater uniformly around the Antarctic coast for ease of reproduction and because climate models simulate different stratification spatial patterns around Antarctica[54]. A uniform flux would therefore make results more comparable when we assess the multi-model impact of the freshwater flux for use in IPCC projections. The impact of spatially-varying meltwater flux on the climate compared to a uniform flux is therefore beyond the scope of our study.

The 10 freshwater perturbation experiments are branched from a randomly selected subset of the same initial condition perturbations on January 1st 1950 used for the 30 ESM2M Large Ensemble simulations first presented in ref. 64 (see Extended Data Fig. ED6)[64]. These new freshwater perturbation experiments follow the same historical and RCP8.5 concentration pathways boundary conditions[5] that were used for the ESM2M Large ensemble runs, differing only from the earlier

run in their added freshwater perturbation. As stated above, the magnitude of the freshwater perturbation follows the projection of Antarctica ice sheet melt from ref. 4. This set of simulations therefore directly shows the climate impact of adding projected ice sheet and shelf melt to the relevant climate change scenario.

It is important that the climate response to the ice sheet melt is assessed in a fully coupled global model in a climate change scenario, as the sensitivity of the system to freshwater flux will change as the climate warms[44] (see Extended Data Fig. ED7). There are feedbacks in the system that can only be quantified with global coupled climate models. Southern Ocean freshwater affects large-scale ocean dynamics and ocean-atmospheric coupling, which in turn have been shown to influence Southern Ocean stratification, convection and sea ice on multiple timescales[65,66]. Ref. 21, for example, show that a shift in the tropical Hadley circulation influences Southern Ocean stratification and convection. As shown in Fig. 2, Antarctic ice sheet melt results in a persistent northwards shift of the ITCZ and Hadley circulation, which will feedback onto the Southern Ocean stratification. Dynamic sea ice has also been shown to influence sub-surface ocean temperatures. The ocean stratification is key for correctly simulating the time-varying sensitivity (see Extended Data Fig. ED4 and ED7) of freshwater-forced subsurface coastal warming, since the main driving term is isopycnal mixing and stirring. Such processes are captured by well tested CMIP5-class models like ESM2M. The results we present are extremely relevant for CMIP5 and CMIP6 projections, so it is important that they are demonstrated in a CMIP5 model like ESM2M.

Significance testing For significance testing of ensemble mean differences, we test for a 95% confidence level using a pair-wise test. We take the difference between each freshwater-perturbed ensemble member and the unperturbed ensemble member from which the perturbed member was branched. The anomalies in the 10-member mean are significant if the mean anomaly is larger than $1.699\sigma/\sqrt{10}$, where σ is the estimated standard deviation of the ensemble mean.

Time of divergence of ensembles The period when the ensembles diverge, indicated by the green bar in Figs. 1B, 2B, 3A and 4B, is the time during which the two ensembles are statistically different at the 95% confidence level. The standard deviation in this calculation is diagnosed from successive 20-year means of each metric from the respective ensembles. Therefore, the time of divergence does not explicitly depend on the number of ensemble members. Any 20-year mean taken from a single ensemble member of freshwater-forced ensemble during this period is more than 95% likely to be different from the ensemble without freshwater melt.

Estimation of sub-surface warming feedback To estimate the increase in ice shelf melt caused by the freshwater-induced subsurface ocean warming around Antarctica, we remain consistent with the methodology in ref. 4. We use the same parameterization to express ice shelf melt rates, OM, as a function of the ocean temperature around the Antarctic coast at 400m depth, T_O:

$$OM = \frac{K_T \rho_W C_W}{\rho_i L_f} |T_O - T_f| (T_O - T_f), \tag{1}$$

where T_f is the freezing point temperature at the ice shelf base, and the combination of physical parameters[4] $(K_T \rho_W C_W)/(\rho_i L_f)$ is equal to 0.224 m yr^{-1} °C^{-2}. The calculation gives a melt rate in m/yr. To convert this melt rate to freshwater flux, we scale the melt rate by the ice shelf surface

area to be consistent with the data in Table 1 in ref. 68. We do this calculation using T_O from the standard RCP8.5 ensemble, as well as the freshwater-forced ensemble. The difference in freshwater flux between the two ensembles then gives the increase in freshwater flux that results from the ice melt-induced sub-surface warming. This freshwater flux does not include the freshwater flux across the grounding line, which is the only flux that contributes towards increased sea level. However, increased shelf melt is likely to lead to an increase in grounding line flux due to a reduction in buttressing[67].

Over the period 1995-2009, this calculation gives a basal melt rate anomaly that is $40\pm10\%$ of the total melt rate, including calving, which is consistent with recent observational estimates of $52\pm14\%$, albeit on the low end[68]. The total basal melt over the period 1995-2009 is 1677 ± 771 Gt/yr, which agrees roughly with the range of observational estimates (1325 ± 235 Gt/yr [41], and 1454 ± 174 Gt/yr [68]). The resulting total cumulative freshwater flux for these calculations, expressed as equivalent global mean sea level (GMSL) rise, is shown in Extended Data Fig. ED7.

We stress that the calculation shown in Extended Data Fig. ED5 is a rough estimate, and that a coupled ice sheet-ocean-atmosphere model simulation is needed to fully assess the magnitude of the sub-surface warming feedback. While our simulations do not resolve ice-shelf cavity dynamics, global atmosphere-ocean feedbacks are necessary to simulate the sensitivity of the sub-surface temperature to freshwater flux (as shown by Fig. ED7), which only a comprehensive climate model like ESM2M can capture. Our calculation assumes a constant ice-shelf area, and it assumes that the total freshwater flux is linearly dependent on the mean melt rate (OM), and does not account

for coastal and ice-shelf cavity dynamics.

For studies that require the detailed knowledge of spatial patterns of sub-ice-shelf melting, other parameterizations are more appropriate[69]. However, the goal of our study is to quantify the net Antarctic sensitivity of ice-shelf melt to the freshwater-induced ocean warming. For such integrated quantities, the detailed knowledge of the melting spatial distribution is less important. Numerous modeling studies focused on the sensitivity of area-averaged melt-rates to the ocean temperature [70–73] have demonstrated that our parameterization adequately captures the melt-rate dependence on temperature. It is this dependence of temperature that drives the area-integrated feedback, so for this purpose, the parametrization is appropriate.

To account for the effects of coastal and ice-shelf dynamics, ref. 4 multiply the melt rate OM by a dimensionless constant. For our uncertainty range, we run additional simulations where we apply half and double the prescribed ref. 4 flux to the transient RCP8.5 simulation in 3 ensemble members each. The sub-surface warming in each case is shown in Extended Data Fig. ED9. Doubling the freshwater flux causes a roughly 28% increase in the freshwater-induced subsurface warming anomaly, and halving it causes a 25% reduction. On the lower end, despite the freshwater flux being reduced by half, the freshwater-induced subsurface warming is still much larger than in the standard RCP8.5 scenario. We then apply this transient simulated relative increase (decrease) in warming compared to the main projected ref. 4 freshwater flux scenario as an upper (lower) bound for ACT anomalies in the feedback calculation. We use a range of the freezing point temperatures, $-1.8^{\circ} < T_f < -2.6^{\circ}$C, and we account for the uncertainty in conversion from ice-shelf melt rate

in m/yr to a freshwater flux based on the numbers in ref. 4. Despite the uncertainty range in our estimate, the freshwater-forced ACT is significantly different from the standard RCP8.5 ensemble. This difference is due to the overall large magnitude of the projected ACT anomaly, which could only be captured in a global climate model.

Seasonal sea ice anomalies Figures ED3A and ED3B show the February and September sea ice area anomalies, respectively. Similar to the annual mean SHI described in the main text, the maximum September SHI anomaly is simulated mid-century, but the February maximum is simulated around the year 2025. The maximum September mean SHI anomaly is $24\pm3\%$ of the pre-industrial SHI, while the February maximum SHI anomaly is $117\pm20\%$ of the pre-industrial February mean.

In February, ESM2M has a generally low total summer sea ice area (around 0.19 million km^2), which is also the reason for the weak 39-year trends compared to the observational trends, shown in Figs. ED3C and ED3D. However, for both February and September SHI trends, the freshwater-forced ensemble is more consistent with the observed trends.

Sensitivity to base state The climate response to ice sheet melt should be assessed in a climate change scenario, since the sensitivity to the freshwater flux will vary as the climate changes. For this reason, we add the ref. 4 estimate to a full RCP8.5 scenario[4]. To demonstrate the importance of the base state, we ran two additional 50 year ensembles with ESM2M, each forced with a constant 0.1 Sv freshwater flux around the Antarctic coast. One set is initiated in the year 1980 and run for 50 years, and the second is initialized in the year 2050 and also run for 50 years. Each of these 5-member ensembles therefore experiences the same freshwater flux for the same duration,

but over a different period in the RCP8.5 scenario. Figure ED7 shows the time evolution of the surface air temperature (SAT), hemispheric precipitation difference (PRE), Antarctic sea ice area (SHI) and sub-surface coastal warming (ACT) metrics in these ensembles compared to the standard RCP8.5 ensemble. The magnitude of the freshwater-induced anomaly is different in each period. The SAT and SHI metrics show a reduced sensitivity in warmer climates, while the ACT shows a larger sensitivity to the freshwater flux. The overall time-dependent anomalies for each of these metrics discussed in the main text therefore depends on both the time-varying freshwater flux and sensitivity to the base state.

Heat budget The heat flux diagnostics (shown in Fig. ED4) that we used for this study are those described in ref. 74. The heat flux terms named 'submescoscale' refers to advection by parameterized sub-grid scale eddies[74]. 'Overflow' refers to the heat transport by along-topography overflow parameterizations. 'Vertical mixing' including both heat fluxes due to convective mixing and vertical diffusion. 'Isopycnal transport' includes parameterized eddy diffusion and eddy-induced advection by mesoscale eddies transporting tracers along surfaces of constant density. The heat flux anomalies were diagnosed in the 5-member ensemble simulation with a constant freshwater flux of 0.1 Sv over the period 1980-2030. Over this 50-year period, we find that the dominant contribution to the freshwater-induced coastal warming averaged between 400 and 700m is the isopycnal transport term (Fig. ED4C), which is largely due to the eddy-induced advection term.

Simulated polynyas Five of the 30 ensemble members of the unperturbed ESM2M ensemble simulate open-ocean polynyas in the period 1970-2020. For the 10 members used to branch off the

freshwater simulations, we chose two of the polynya members and eight non-polynya members to represent the ensemble as whole (as shown in Fig. ED6).

We tested whether there is a difference in the response of the simulations derived from polynya-members versus the ones without polynyas, and we find no significant difference. For example, we examined the 1979-2017 sea ice trends discussed in section 3 of the paper, and shown in Fig. 3B, which are likely to be most affected by the simulated polynyas (as shown by the spread in sea ice extent over this period in Fig. ED6). The linear trends in the 2 freshwater simulations derived from polynya members are 0.029 and -0.0087 $\times 10^6$ km^2/yr, indicating no significant bias as they lie both above and below the mean of the distribution (0.015 $\times 10^6$ km^2/yr). There is one freshwater-perturbed member that simulates several years of convection in this period, resulting in a large negative trend in sea ice area of -0.042 $\times 10^6$ km^2/yr, as shown in Fig. 3B. However, this is not a simulation derived from an ensemble member that simulates a polynya in the unperturbed RCP8.5 scenario. Therefore, the presence of polynyas in some members of the unperturbed ensemble does not affect the response.

The presence of long-term polynya's simulated over the historical period in 5 of the 30 standard ensemble members is not supported by observations. However, none of the freshwater-forced ensemble members simulate such long-term events. It therefore seems that ESM2M (and likely CMIP5 models as a whole) is more prone to simulating large convective events compared to observations, perhaps because it lacks the appropriate freshwater flux in the unperturbed simulations.

ESM2M Southern Ocean evaluation In this section, we provide a comparison of the Southern Ocean density structure around the Antarctic coast in ESM2M with the 2008-2012 Southern Ocean State Estimate (SOSE, iteration 105)[63]. The density structure is important for simulating the appropriate sub-surface warming response to the meltwater flux. SOSE is a state estimate based on the MITgcm, constrained using available data. In particular, SOSE uses Argo and seal data to constrain the solution near the Antarctic coast. While SOSE is a model simulation, it provides an estimate of the Southern Ocean that is consistent with available observations.

Extended Data Fig. ED10A shows the ESM2M mean state mixed layer depth, the pattern of which roughly agrees with estimates from observations[59]. Extended Data Fig. ED10B shows vertical density profiles for ESM2M (black) and SOSE (red) over three key regions where meltwater-induced subsurface warming is simulated: 1. the Ross Sea, 2. the Weddell Sea and 3. Eastern Antarctica. These profiles show that the overall density structure and stratification around the Antarctic coast in ESM2M is similar to the data-constrained SOSE. While ESM2M has a light overall bias, the vertical stratification is similar to SOSE. Extended Data Fig. ED10C shows Southern Ocean zonal mean ESM2M and SOSE isopycnal surfaces of constant density (solid and dashed respectively), as well as locally in the numbered regions defined above. South of 60°S, the ESM2M and SOSE density structures are very similar, indicating that the meltwater-induced temperature anomaly should be reasonably well-represented in our simulations. However, ESM2M has a weaker isopycnal slope away from the coast compared to SOSE. This difference likely means that the meltwater-induced temperature anomaly is less confined to the coast in ESM2M than it would be given the SOSE density structure. While this could lead to an underestimation of the

warming, the figures show that the warming is mostly confined around the coast where isopycnals are mostly similar to SOSE.

49. Gent, P. R. et al. The Community Climate System Model Version 4. Journal Of Climate **24**, 4973-4991 (2011).

50. Dunne, J. P. et al. GFDL's ESM2 Global Coupled Climate-Carbon Earth System Models. Part I: Physical Formulation and Baseline Simulation Characteristics. Journal Of Climate **25**, 6646-6665 (2012).

51. Dunne, J. P. et al. GFDL's ESM2 Global Coupled Climate-Carbon Earth System Models. Part II: Carbon System Formulation and Baseline Simulation Characteristics. Journal Of Climate **26**, 2247-2267 (2013).

52. Griffies, S. The Gent-McWilliams skew flux. Journal Of Physical Oceanography **28**, 831-841 (1998).

53. Stocker, T. et al. Technical Summary, book section TS, 33-115 (Cambridge University Press, Cambridge, United Kingdom and New York, NY, USA, 2013). URL `www.climatechange2013.org`.

54. Sallee, J. B. et al. Assessment of Southern Ocean water mass circulation and characteristics in CMIP5 models: Historical bias and forcing response. Journal Of Geophysical Research-Oceans **118**, 1830-1844 (2013).

55. Shu, Q., Song, Z. & Qiao, F. Assessment of sea ice simulations in the CMIP5 models. Cryosphere **9**, 399-409 (2015).

56. Reintges, A., Martin, T., Latif, M. & Park, W. Physical controls of Southern Ocean deep-convection variability in CMIP5 models and the Kiel Climate Model. Geophysical Research Letters **44**, 6951-6958 (2017).

57. Gordon, A. Deep Antarctic Convection West Of Maud Rise. Journal Of Physical Oceanography **8**, 600-612 (1978).

58. de Lavergne, C., Palter, J. B., Galbraith, E. D., Bernardello, R. & Marinov, I. Cessation of deep convection in the open Southern Ocean under anthropogenic climate change. Nature Climate Change **4**, 278-282 (2014).

59. Pellichero, V., Sallee, J.-B., Schmidtko, S., Roquet, F. & Charrassin, J.-B. The ocean mixed layer under Southern Ocean sea-ice: Seasonal cycle and forcing. Journal of Geophysical Research-Oceans **122**, 1608-1633 (2017).

60. Swart, N. C. & Fyfe, J. C. Observed and simulated changes in the southern hemisphere surface westerly wind-stress. Geophysical Research Letters **39**, L16711 (2012).

61. Downes, S. M. & Hogg, A. M. Southern Ocean Circulation and Eddy Compensation in CMIP5 Models. Journal of Climate **26**, 7198-7220 (2013).

62. Frölicher, T. L. et al. Dominance of the Southern Ocean in Anthropogenic Carbon and Heat Uptake in CMIP5 Models. Journal Of Climate **28**, 862-886 (2015).

63. Verdy, A. & Mazloff, M. R. A data assimilating model for estimating Southern Ocean biogeochemistry. Journal of Geophysical Research-Oceans **122**, 6968-6988 (2017).

64. Rodgers, K. B., Lin, J. & Froelicher, T. L. Emergence of multiple ocean ecosystem drivers in a large ensemble suite with an Earth system model. Biogeosciences **12**, 3301-3320 (2015).

65. Wang, Z. et al. An atmospheric origin of the multi-decadal bipolar seesaw. Scientific Reports **5**, 8909 (2015).

66. Meehl, G. A., Arblaster, J. M., Bitz, C. M., Chung, C. T. Y. & Teng, H. Antarctic sea-ice expansion between 2000 and 2014 driven by tropical Pacific decadal climate variability. Nature Geoscience **9**, 590-595 (2016).

67. Dupont, T. & Alley, R. Assessment of the importance of ice-shelf buttressing to ice-sheet flow. Geophysical Research Letters **32**, L04503 (2005).

68. Depoorter, M. A. et al. Calving fluxes and basal melt rates of Antarctic ice shelves. Nature **502**, 89-92 (2013).

69. Lazeroms, W. M. J., Jenkins, A., Gudmundsson, G. H. & van de Wal, R. S. W. Modelling present-day basal melt rates for Antarctic ice shelves using a parametrization of buoyant meltwater plumes. Cryosphere **12**, 49-70 (2018).

70. MacAyeal, D. R. Evolution of tidally triggered meltwater plumes below ice shelves, in: Oceanology of the Antarctic Continental Shelf, edited by: Jacobs, S, 133-143 (American Geophysical Union, Washington, D. C., 1985).

71. Holland, P. R., Jenkins, A. & Holland, D. M. The response of ice shelf basal melting to variations in ocean temperature. Journal of Climate **21**, 2558-2572 (2008).

72. Little, C. M., Gnanadesikan, A. & Oppenheimer, M. How ice shelf morphology controls basal melting. Journal of Geophysical Research-Oceans **114**, C12007 (2009).

73. Goldberg, D. N. et al. Investigation of land ice-ocean interaction with a fully coupled ice-ocean model: 2. Sensitivity to external forcings. Journal of Geophysical Research-Earth Surface **117**, F02038 (2012).

74. Griffies, S. M. Elements of the modular ocean model (mom) (tech. rep. 7, 618 pp.). NOAA Geophysical Fluid Dynamics Laboratory Ocean Group (2012).

75. NOAA, National Geophysical Data Center, Boulder, Colorado, 1988. ETOPO5, Data Announcement 88-MGG-02, Digital relief of the Surface of the Earth.

Data availability

GFDL ESM2M model code is publicly available from `https://github.com/mom-ocean` and the results from the standard RCP8.5 ensemble and freshwater forced RCP8.5 ensemble simulations are freely available from the corresponding author. The prescribed RCP8.5 freshwater flux used in this paper is available from ref. 4. Antarctic sea ice extent from satellite measurements is available from the National Snow and Ice Data Center. The Southern Ocean State Estimate data used for model evaluation is available from `http://sose.ucsd.edu/bsose_solution_Iter105.html`. Topographical data used in Figs. 1-2, 4, and Extended Data Figs. ED1, ED9, and ED10 is available in MATLAB and is provided by NOAA[75].

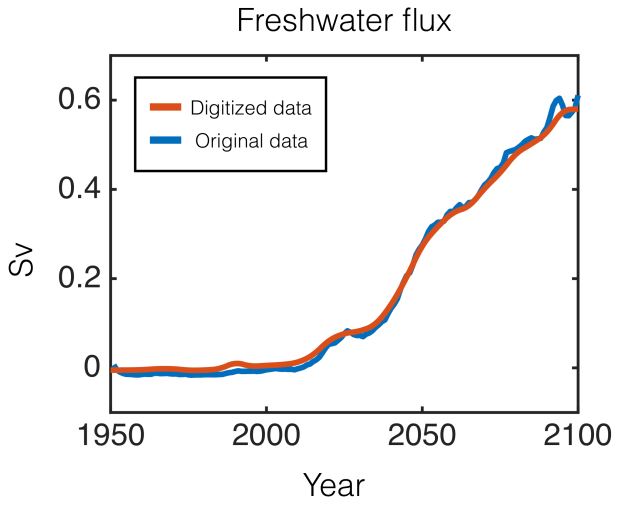

Figure ED1: **Applied RCP8.5 freshwater flux**: The orange line shows the digitized data applied to ESM2M and the blue line shows the original data from ref. 4 (1 Sv = 10^6 m^3/s).

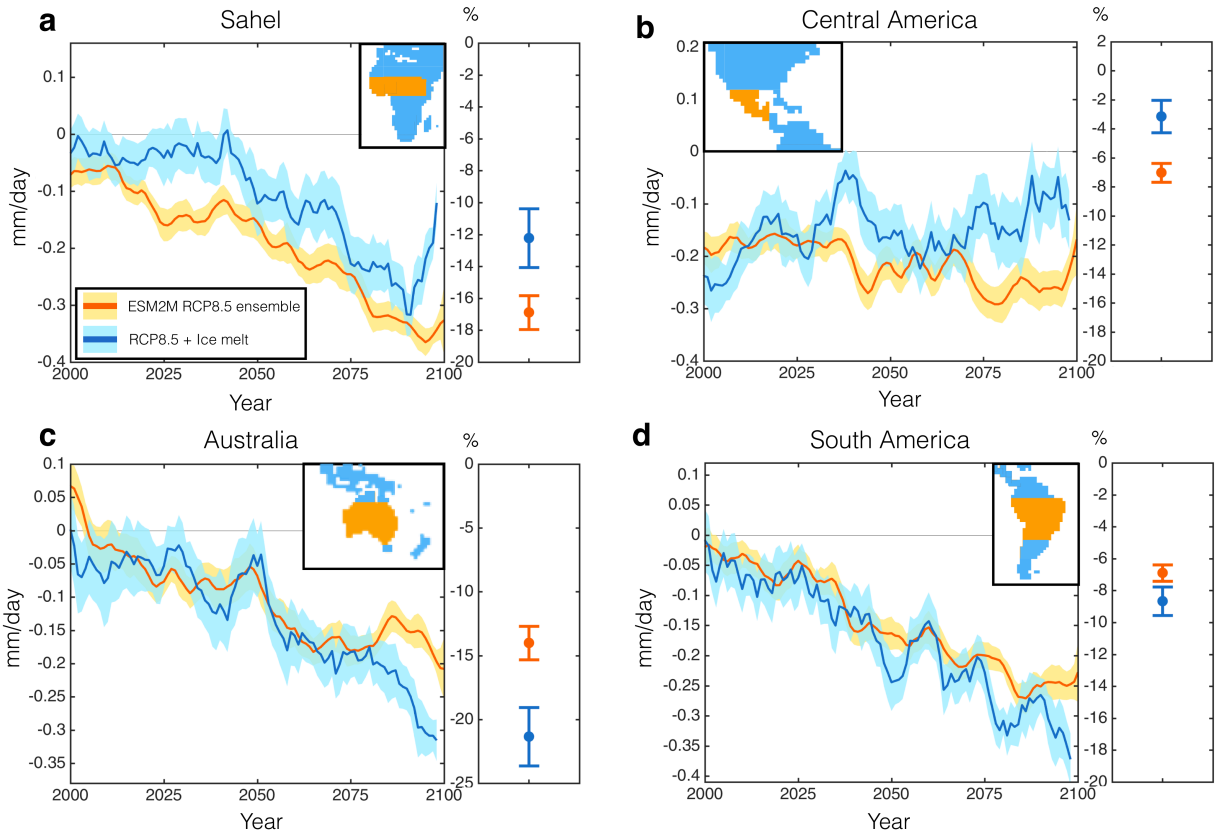

Figure ED2: **Regional area mean precipitation-evaporation anomalies**: Anomalies are shown as a function of time for **a**, the Sahel, **b**, Central America, **c**, Australia and **d**, South America. Orange shows the standard RCP8.5 30-member ESM2M ensemble and blue shows the 10-member RCP8.5 with added time-varying freshwater melt around Antarctica. The solid lines show the ensemble means and the shading shows the 95% uncertainty in the mean. The data points on the right of each panel shows the 2080-2100 mean anomalies, expressed as a percentage relative to the pre-industrial mean state, with the error bars showing the 95% uncertainty in the means. Here, the anomalies are calculated with respect to the pre-industrial control simulation. The map inset panels indicate the area over which the respective anomalies are calculated. All time series are smoothed with a 5-year filter.

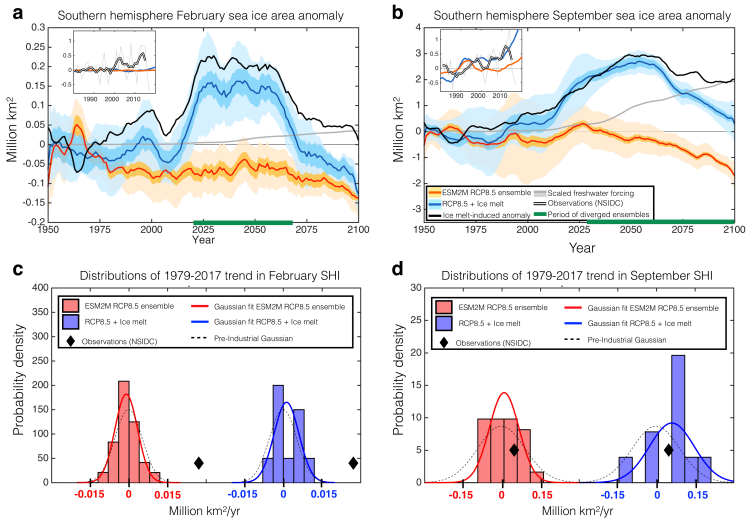

Figure ED3: **Seasonal sea ice anomalies**: Time series of the **a**, February and **b**, September Southern Hemisphere sea-ice (SHI) anomaly relative to the 1950-1970 mean. Orange shows the standard ensemble and blue shows the meltwater ensemble. Solid lines show ensemble means, the dark shading shows the uncertainty in the mean and the light shading shows the full ensemble spread of 20-year SHI means. The solid black line shows the difference between the orange and blue lines, and the applied meltwater flux is shown in grey (scaled to the final 5-year mean of the meltwater-induced SHI anomaly). The green bar indicates when the full ensembles have diverged. The inset panels shows the 1980-2020 period with the double black line showing respective monthly mean observed sea ice area from the National Snow and Ice Data Center, relative to the 1980-2000 mean. The thin grey line shows the unsmoothed observations. **c**-**d**, Distribution of linear trends in SHI over the period 1979-2017, calculated for each ensemble member, for February (**c**) and September (**d**) means. The red bars show the standard RCP8.5 ensemble and blue bars show the freshwater ensemble, with different x-axes. The solid lines show Gaussian fits to the distributions, and the dashed black line shows the pre-industrial distribution. The observations are shown in black diamonds.

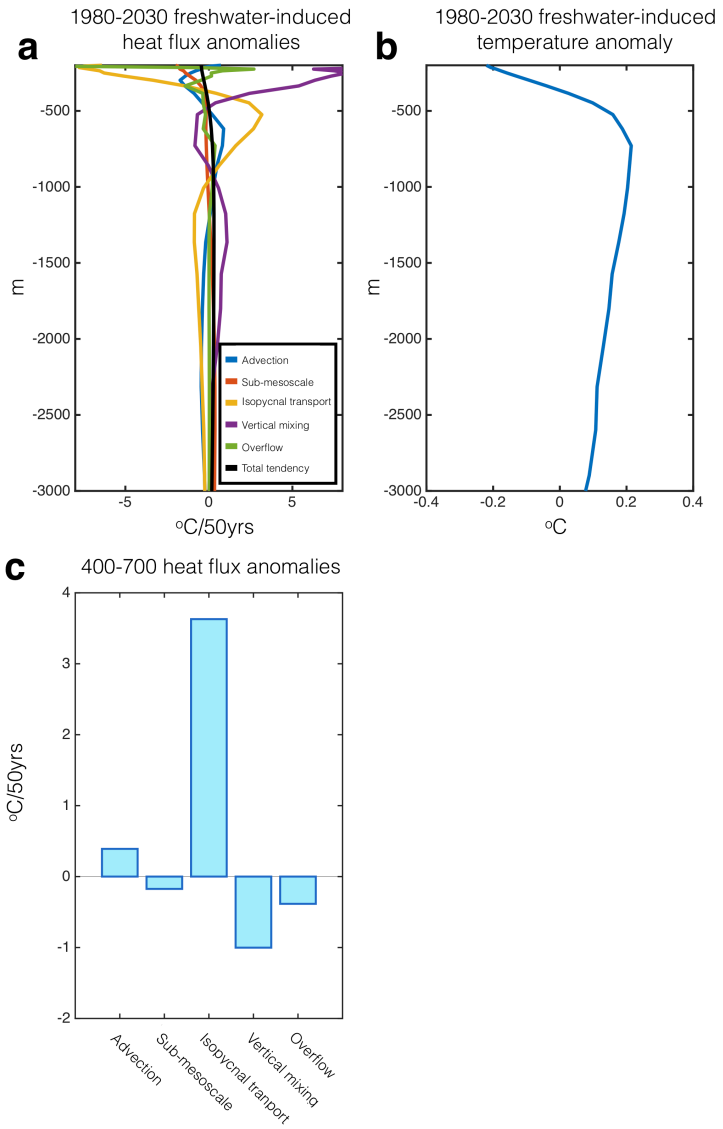

Figure ED4: **Heat budget analysis**: 1980-2030 freshwater-induced **a**, heat flux anomalies and **b**, temperature anomaly averaged along the Antarctic coast due to a 0.1 Sv (1 Sv = 10^6 m^3/s) freshwater perturbation. **c**, 1980-2030 mean freshwater-induced heat flux anomalies averaged between 400-700m depth along the Antarctic coast. All anomalies shown here are calculated relative to the mean of the 30-member RCP8.5 ensemble without ice sheet melt.

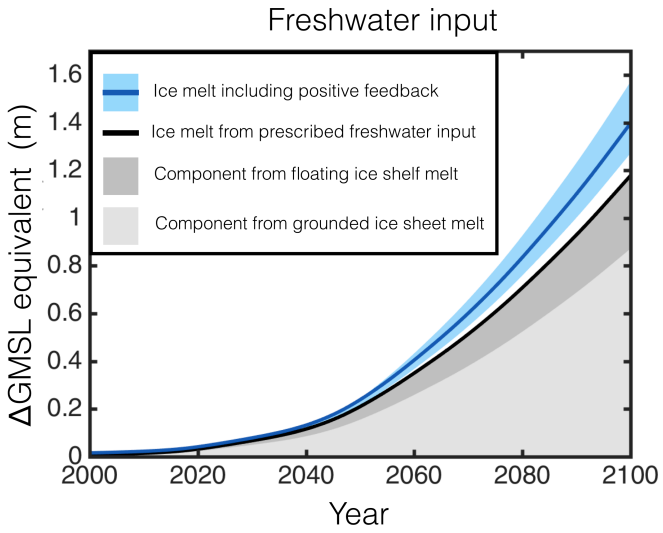

Figure ED5: **Ice-melt feedback**: Ice melt freshwater input, in global mean sea level equivalent, due to the RCP8.5 prescribed meltwater (black). The dark and light grey shadings show the components of the prescribed flux from ice shelf and ice sheet melt respectively. Only the ice sheet melt contributes towards sea level. The blue line shows the total freshwater flux including the prescribed flux as well as the estimated feedback associated with ice shelf melt from the freshwater-induced ocean warming. The blue shading shows the 95% uncertainty range.

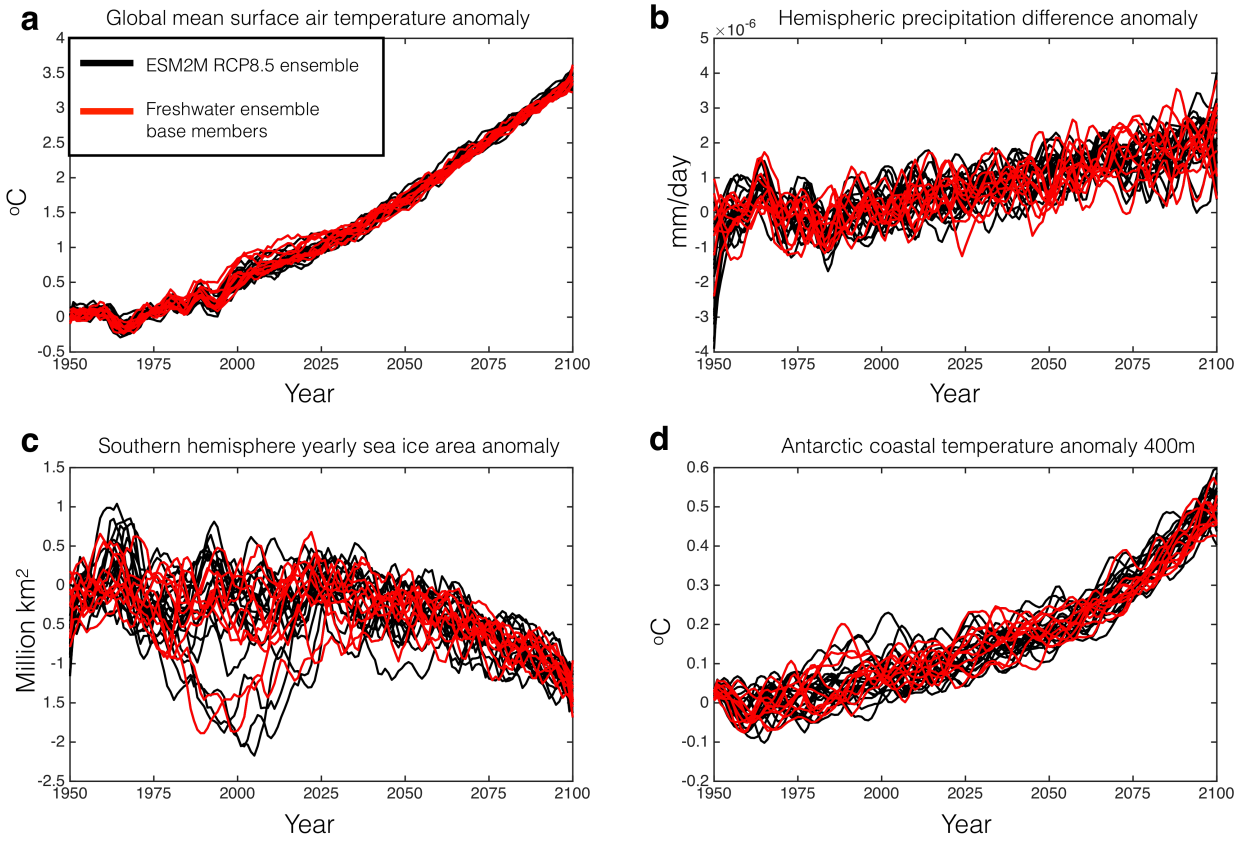

Figure ED6: **Selection of ensemble members for meltwater experiments**: Time series of **a**, global mean surface air temperature (SAT), **b**, north-south hemispheric precipitation difference (PRE), **c**, Annual mean Southern Hemisphere sea ice area (SHI) and **d**, Antarctic coastal ocean temperature at 400m depth (ACT) anomalies in the 30-member standard RCP8.5 scenario relative to the pre-industrial control. The black lines show all 30 ensembles members and the red lines show the unperturbed ensemble members used for the freshwater forced simulations.

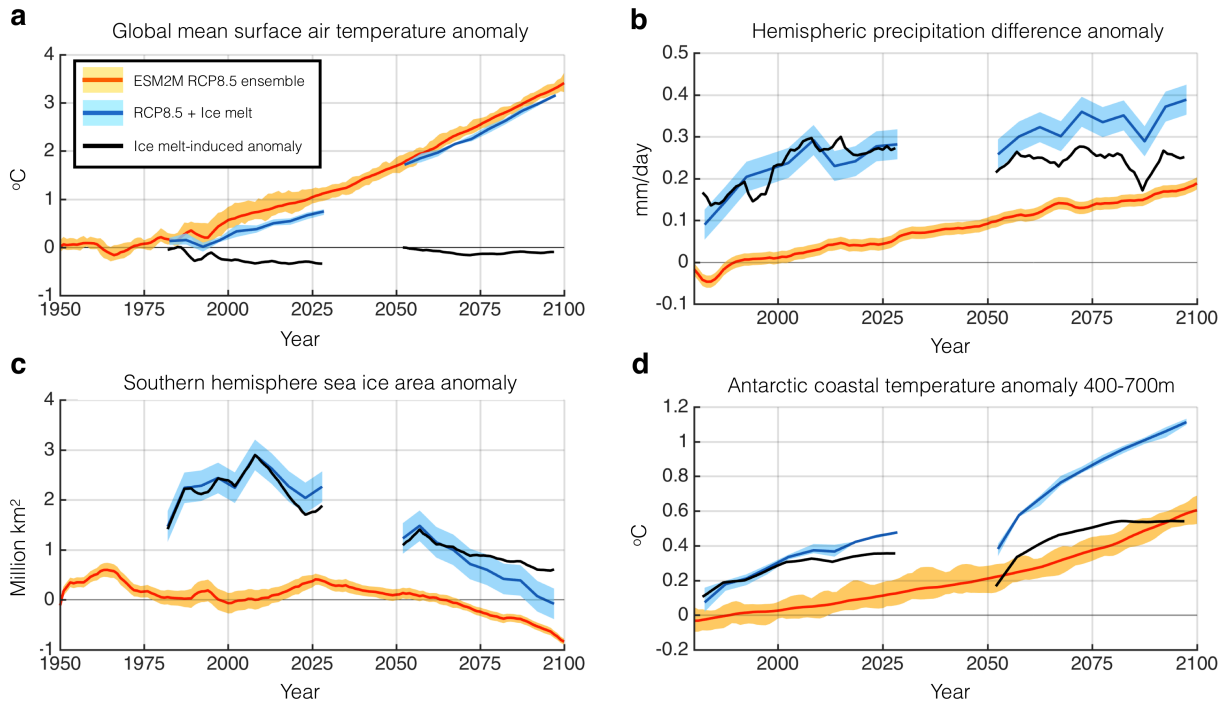

Figure ED7: **Sensitivity to base state**: Time series of **a**, the global mean surface air temperature anomaly, **b**, North-South hemispheric precipitation difference anomaly **c**, Southern hemisphere sea ice area anomaly and **d**, ocean temperature anomaly around the Antarctic coast averaged between 400-700m depth, relative to the pre-industrial control. Orange shows the yearly standard RCP8.5 ensemble and blue shows the 5-year means of the 5-member freshwater ensembles. The freshwater ensembles in these experiments are hosed with 0.1 Sv for 50 years in two separate periods: 1980-2030 and 2050-2100 (1 Sv = 10^6 m^3/s). The freshwater ensembles in each period are initialized from the year 1980 and 2050 from the standard RCP8.5 ensemble, respectively. Each period is shown as a separate line. Solid lines show ensemble means, the dark shading shows the 90% uncertainty in the mean. The solid black line in each panel shows the difference between the freshwater-forced and standard RCP8.5 ensemble

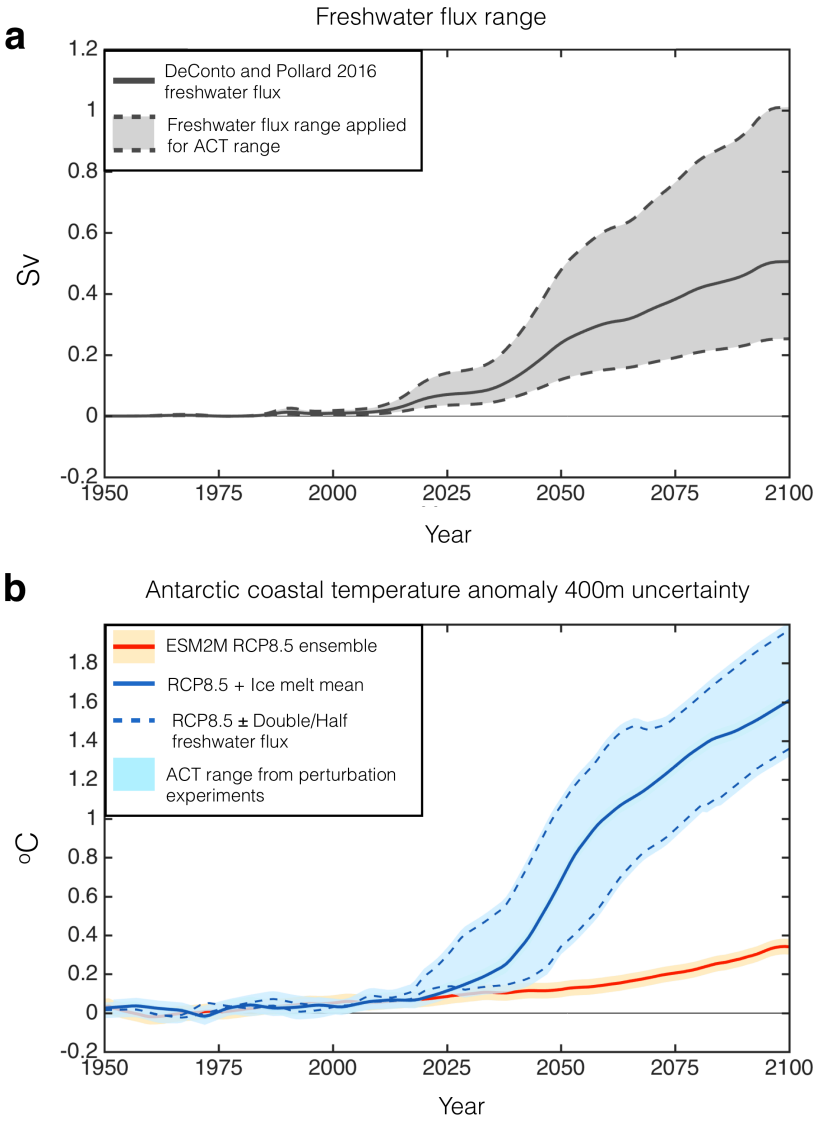

Figure ED8: **Range of 400m ocean warming**: **a**, Range of freshwater flux. The solid grey line shows the projected flux from ref. 4 and the dashed lines and shading show the same flux, but multiplied by factor of 0.5 and 2 (1 Sv = 10^6 m^3/s). **b**, Antarctic coastal 400m ocean temperature anomalies in the standard ensemble (red) and in the meltwater ensembles: the solid blue line shows the response to the projected flux from ref. 4, and the dashed blue lines show the temperature range covered by the $0.5\times$ and $2\times$ flux experiments. The $0.5\times$ and $2\times$ flux experiments have 3 ensemble members each. The shading shows the full ensemble spread of 20-year means.

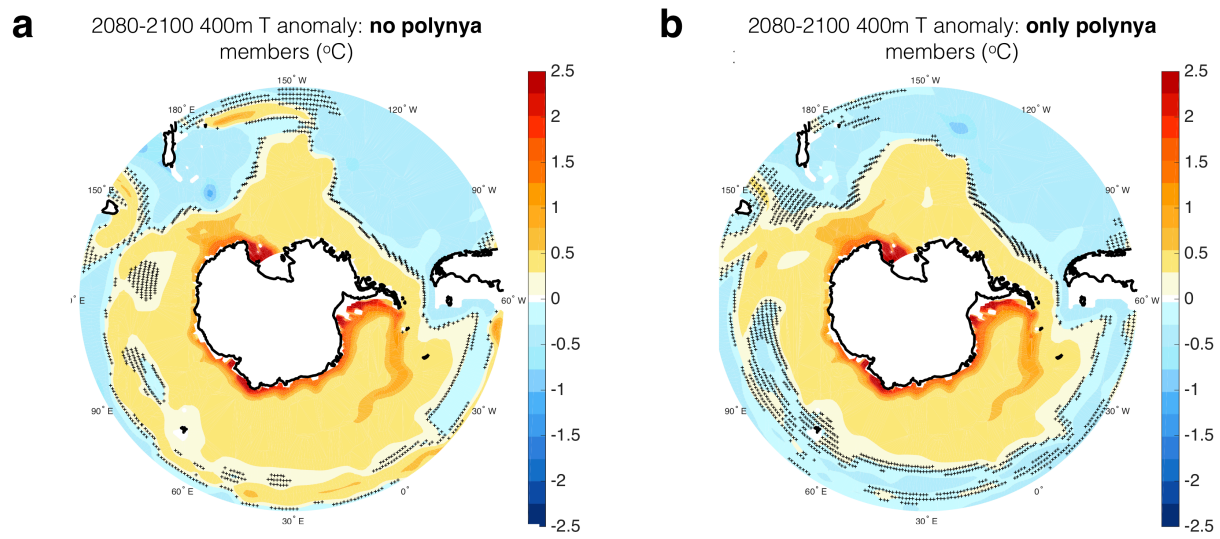

Figure ED9: **Warming response of polynya and non-polynya members**: 2080-2100 meltwater-induced anomaly of the ocean temperature around the Antarctic coast at 400m depth in the meltwater ensemble members branched off the **a**, 8 non-polynya and **b**, 2 (open ocean Weddell Sea) polynya members from the standard ensemble. Anomalies are pair-wise calculated relative to the unperturbed ensemble members. Hatching indicates where the anomalies are not significant at the 95% level.

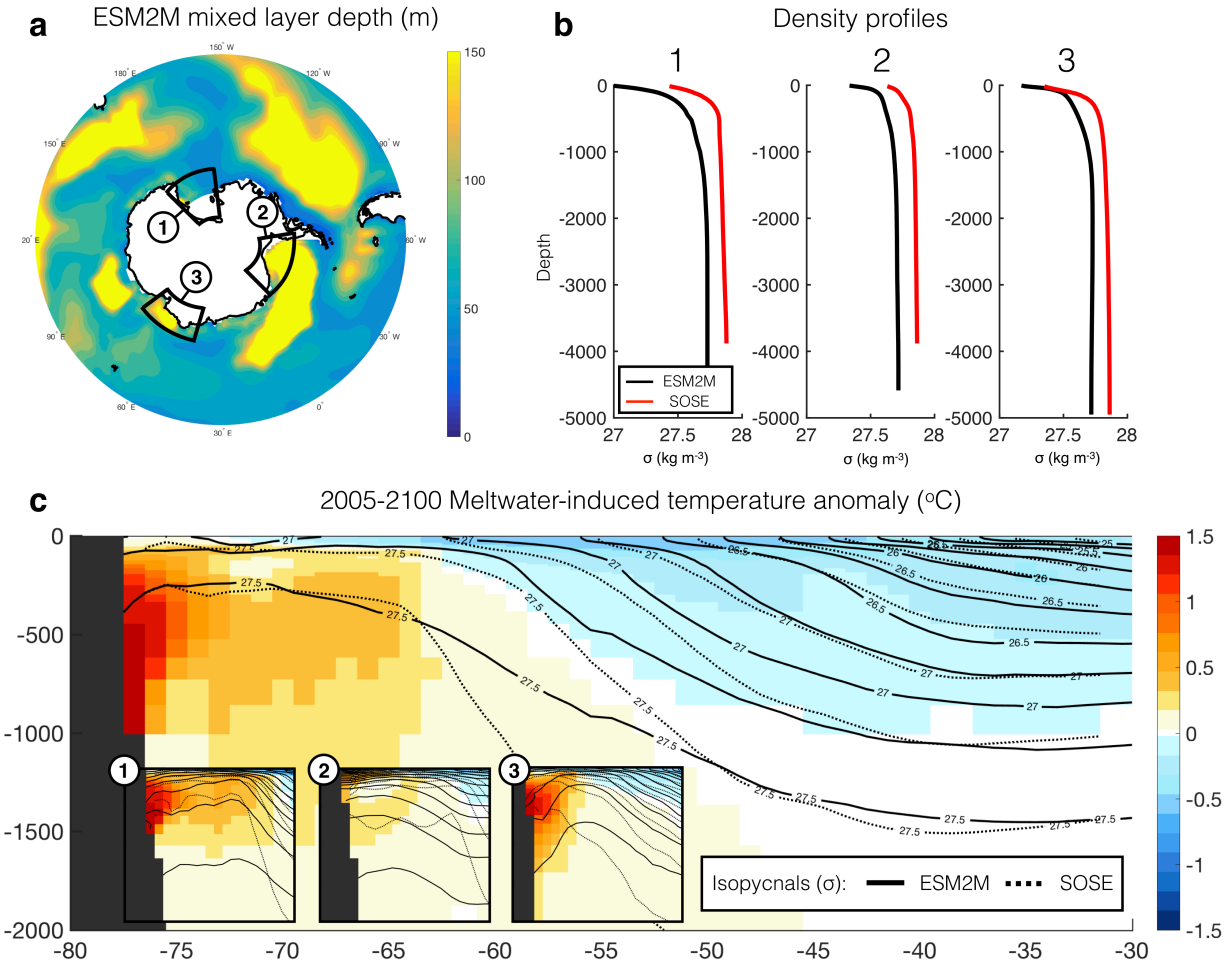

Figure ED10: **ESM2M-Southern Ocean State Estimate (SOSE) comparison**: **a**, ESM2M pre-industrial annual mean state mixed layer depth. **b**, Area-mean density profiles for ESM2M (black) and SOSE (red) for each of the numbered boxes in panel A. **c**, ESM2M 2005-2100 mean meltwater-induced temperature anomaly (zonal mean), as well as zonal mean ESM2M and SOSE isopycnal surfaces (solid and dashed respectively). The numbered inset panels in panel C are zoomed in on the similarly numbered regions from panels A, showing the upper 2000m of the ocean, between 80°S and 60°S in regions 1 and 2, and 70°S to 50°S in region 3).